Electronic Supplementary Material (ESI) for Environmental Science: Nano.

Supporting Information for

UV-induced aggregation of polystyrene nanoplastics: Effects of radicals, surface functional groups and electrolyte

Xinjie Wang [a], Yang Li [a*], Jian Zhao [a], Xinghui Xia [a], Xiaonan Shi [b], Jiajun Duan [a], Wen Zhang [b]

[a] *Key Laboratory of Water and Sediment Sciences of Ministry of Education, State Key Laboratory of Water Environment Simulation, School of Environment, Beijing Normal University, Beijing 100875, People's Republic of China*

[b] *John A. Reif, Jr. Department of Civil and Environmental Engineering, New Jersey Institute of Technology, Newark, New Jersey, 07102, USA*

Supporting information contains:

Number of pages: 18

Figures: S1-S13

Tables: S1-S5

S1. Experimental Setup

The reaction unit in a 50-mL beaker was placed under a UV lamp with a distance of 25 cm between the UV lamp and the suspension surface to obtain a UV intensity of 0.4 mW·cm^{-2}. The liquid suspension in the beaker was continuously mixed and transferred between the reaction unit and the measurement liquid cell placed inside DLS instrument through the whole aggregation period.

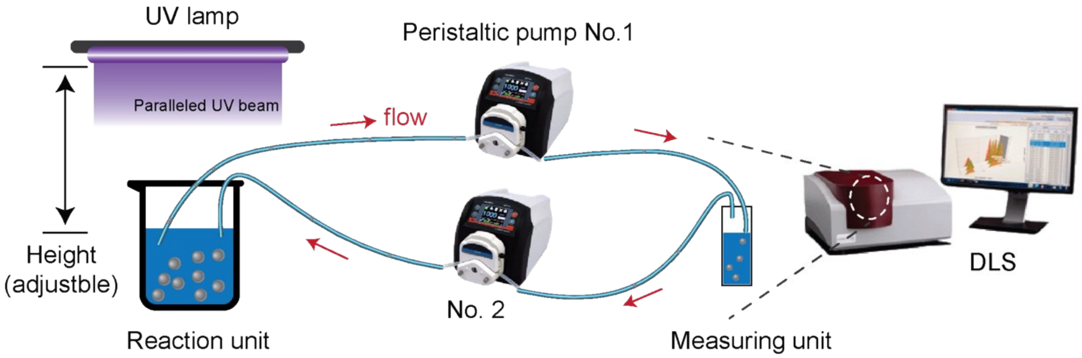

Fig. S1 Schematic of the experimental setup for the continuous measurement of the hydrodynamic diameter of PSNPs in water under UV irradiation.

S2. Calculation Method for the Attachment Efficiencies (α) of the Three PSNPs

The initial aggregation rate constant of PSNPs (*k*) is proportional to the inverse of PSNP concentration (N_0) and the initial increase rate of the hydrodynamic diameter (D_h) with time (*t*) are calculated by eq S1.[1]

$$k \propto \frac{1}{N_0}\left(\frac{dD_h(t)}{dt}\right)_{t\rightarrow 0} \tag{S1}$$

The hydrodynamic diameter (D_h) was obtained by the above-mentioned DLS measurement for the PSNP suspensions. The attachment efficiencies (α) of three PSNPs were calculated by normalizing the *k* of a given solution chemical condition by the k_{fast} of a favorable (non-repulsive) aggregation condition.[2] Because all aggregation experiments used the same initial concentrations of PSNPs, the values of α are calculated by eq S2:

$$\alpha = \frac{k}{k_{fast}} = \frac{\frac{1}{N_0}\left(\frac{dD_h(t)}{dt}\right)_{t\rightarrow 0}}{\frac{1}{(N_0)_{fast}}\left(\frac{dD_h(t)}{dt}\right)_{t\rightarrow 0,\, fast}} = \frac{\left(\frac{dD_h(t)}{dt}\right)_{t\rightarrow 0}}{\left(\frac{dD_h(t)}{dt}\right)_{t\rightarrow 0,\, fast}} \tag{S2}$$

where the subscript "fast" represents a favorable aggregation condition. The numerator and denominator were referred to the aggregation rate constants under the reaction-limited aggregation regime (RLA, α<1) and the diffusion limited aggregation regime (DLA, α=1), respectively.[3]

S3. Equations and Parameters Used for DLVO and eDLVO Calculations

For uncoated PSNPs, the total interaction energy (U_{TOTAL}) equals to the sum of van der Waals attraction energy (U_{VDW}) and the electrical repulsion energy (U_{EDL}). For PSNPs-NH$_2$, PSNPs-COOH and the three UV-irradiated PSNPs, the total interaction energy equals to the sum of U_{VDW}, U_{EDL}, and the Lewis acid-base interaction energy (U_{AB}). U_{AB} was included to account for the hydrophilic repulsion and acid-base or H-bond interactions between the two approaching PSNPs with surface coatings or after UV exposure.[4, 5] The Hamaker constant is highly affected by the surface properties and functional groups of polystyrene polymer formed in the polymerization process.[6] To make our DLVO and eDLVO calculation more accurately, we have measured the Hamaker constants for three PSNPs based on the reported method.[4, 7] U_{VDW}, U_{EDL}, and U_{AB} can be calculated using the following equations:

$$U_{VDW} = -\left(\frac{A_{131}a}{12h}\right)\left[\frac{1}{1 + \frac{11.12h}{\lambda_c}}\right] \tag{S3}$$

$$A_{131} = 24\pi h_0\left(\sqrt{\gamma_1^{LW}} - \sqrt{\gamma_3^{LW}}\right)^2 \tag{S4}$$

$$U_{131}^{EDL} = 2\pi\varepsilon\varepsilon_0 a\left(\xi^2\exp(-\kappa h) - \frac{1}{2}\xi^2\exp(-2\kappa h)\right) \tag{S5}$$

$$U_{AB} = \frac{\pi a\lambda}{2}\Delta G_{131}^{LW}\exp\left(\frac{h_0 - h}{\lambda}\right) \tag{S6}$$

$$\Delta G_{131}^{LW} = 4\left(\sqrt{\gamma_1^{+}\gamma_3^{-}} + \sqrt{\gamma_1^{-}\gamma_3^{+}} - \sqrt{\gamma_1^{+}\gamma_1^{-}} - \sqrt{\gamma_3^{+}\gamma_3^{-}}\right) \tag{S7}$$

For the interfacial tension parameters (i.e., γ^{LW}, γ^{+}, and γ^{-}), the subscript of 1 and

3 represent PSNPs and water, respectively. For water, the values of γ^{LW}, γ^{+}, and γ^{-} are 21.8, 25.5 and 25.5 mJ·m^{-2}, respectively. The values of γ^{LW}, γ^{+}, and γ^{-} for PSNPs were determined by contact angles (θ), which were measured by using three probe liquids with known surface tension parameters:

$$\gamma_i^L(1+\cos\theta) = 2\sqrt{\gamma_i^{LW}\gamma^{LW}} + 2\sqrt{\gamma_i^{+}\gamma^{-}} + 2\sqrt{\gamma_i^{-}\gamma^{+}} \tag{S8}$$

where the subscript *i* represents water (γ^{L}=72.8, γ^{LW}=21.8, and γ^{+}= γ^{-}=25.5 mJ·m^{-2}), glycerol (γ^{L}=64.0, γ^{LW}=34.0, γ^{+}=3.9, and γ^{-}=57.4 mJ·m^{-2}) or formamide (γ^{L}=58.0, γ^{LW}=39.0, γ^{+}=2.3, and γ^{-}=39.6 mJ·m^{-2}). The contact angles of three probe liquids onto flat surfaces made of different PSNPs were measured by a contact angle goniometer (JC2000c, Shanghai, China).[4, 7] PSNPs were coated on clean glass slides by drying concentrated PSNPs suspension.[6] The same Hamaker constant and surface tension parameters were used for pristine PSNPs and 30 min UV-irradiated PSNPs as they had the same contact angles in three probe liquids. The experimentally determined Hamaker constants of three PSNPs have a comparable order of magnitude with those reported previously (2.1× 10^{-18} ~ 6.06 × 10^{-18} mJ).[4, 8, 9]

Table S1 Hamaker constants, contact angles, and surface tension parameters of pristine PSNPs and UV-irradiated PSNPs.

Sample	Hamaker constant, A_{131} (mJ)	Contact angles (°)			Surface tension (mJ·m^{-2})		
		Water	Glycerol	Formamide	γ^{LW}	γ^{+}	γ^{-}
PSNPs/UV-irradiated PSNPs	4.3×10^{-18}	36.9±0.1	43.6±0.2	31.6±0.2	48.4	20.8	26.0
PSNPs-NH_2/UV-irradiated PSNPs-NH_2	3.9×10^{-18}	35.6±0.1	40.2±0.3	30.5±0.3	45.6	24.1	34.2
PSNPs-COOH/UV-	2.9×10^{-18}	25.8±0.1	30.8±0.1	24.8±0.1	38.8	8.0	27.5

irradiated PSNPs-COOH

Note: UV-irradiated PSNPs refers to pristine PSNPs that were irradiated by UV light in DI water after 30 min.

Table S2 Other key parameters used in DLVO and eDLVO calculations.

μ	The radius of polystyrene nanoplastic (PSNPs) (m).
λc	The "characteristic wavelength" of the interaction, often assumed to be 100 nm.
A_{131}	Hamaker constant for interacting subject "1" (PSNPs) in the medium "3" (water). A_{131} was used for U_{VDW} calculation.
	Zeta potentials of PSNPs under different water chemical conditions (mV).
h	The separation distance between two interacting particles (nm).
κ	The inverse Debye length (m^{-1}) defined as $\kappa^{-1} = \left(\frac{\varepsilon\varepsilon_0 k_B T}{2N_A e^2 I}\right)^{1/2} = \left(\frac{\varepsilon\varepsilon_0 k_B T}{N_A{}^2 e^2 \sum c_i z_i{}^2}\right)^{1/2}$
N_A	Avogadro's number, 6.02×10^{23} mol^{-1}.
c_i	The molar concentration of one species ions (i, $mol\cdot L^{-1}$).
ε_0	The dielectric permittivity of a vacuum (8.854×10^{-12} $C\cdot V^{-1}\cdot m^{-1}$).
ε	The dielectric constant of water (78.5, dimensionless).
z_i	The valence of the ith ion.
k_B	Boltzmann's constant (1.38×10^{-23} $J\cdot K^{-1}$).
T	The absolute temperature taken as 298 K.
z	The charge number for the present electrolyte. For NaCl, the charge number is 1.
ΔG_{131}^{LW}	The polar interaction energy, for substance "l" in presence of medium "3" ($mJ\cdot m^{-2}$).
λ	The characteristic decay length of AB interaction in water (0.6 nm).
h_0	The minimum equilibrium distance due to the Born repulsion, 0.156 nm.

S4. Synthesis Routes of the Three PSNPs

1. Sulfate groups at the chain termini are located on the surface of PSNPs, which provided negative surface charge of PSNPs. The surfactants adsorbed on the PSNP surface also rendered PSNPs with negative surface charge.

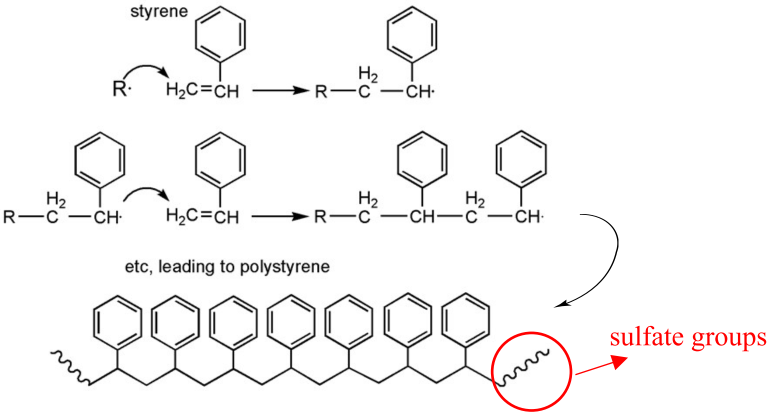

Fig. S2 Schematic of polystyrene nanoplastics production (R• refers to sulfate free radical).

2. PSNPs-NH_2 may have residual surface sulfate groups (negatively-charged) leftover from synthesis with sulfate-based surfactants and initiators. The surfactants adsorbed on the PSNPs-NH_2 surface also rendered PSNPs-NH_2 with negative surface charge.

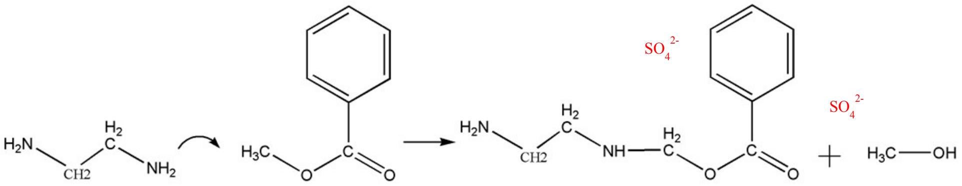

Fig. S3 Schematic of amino-modified polystyrene nanoplastics production.

3. PSNPs-COOH have residual surface sulfate groups (negatively-charged) leftover from synthesis with sulfate-based surfactants and initiators.

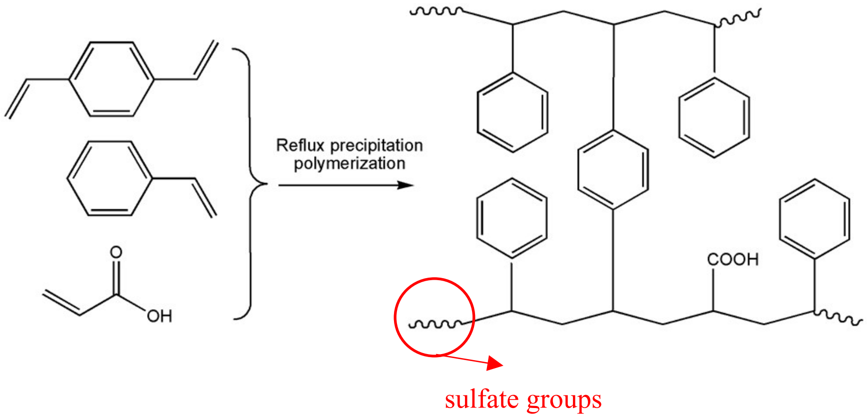

Fig. S4 Schematic of carboxyl-modified polystyrene nanoplastics production.

S5. Interaction Energies between PSNPs in Dark Conditions

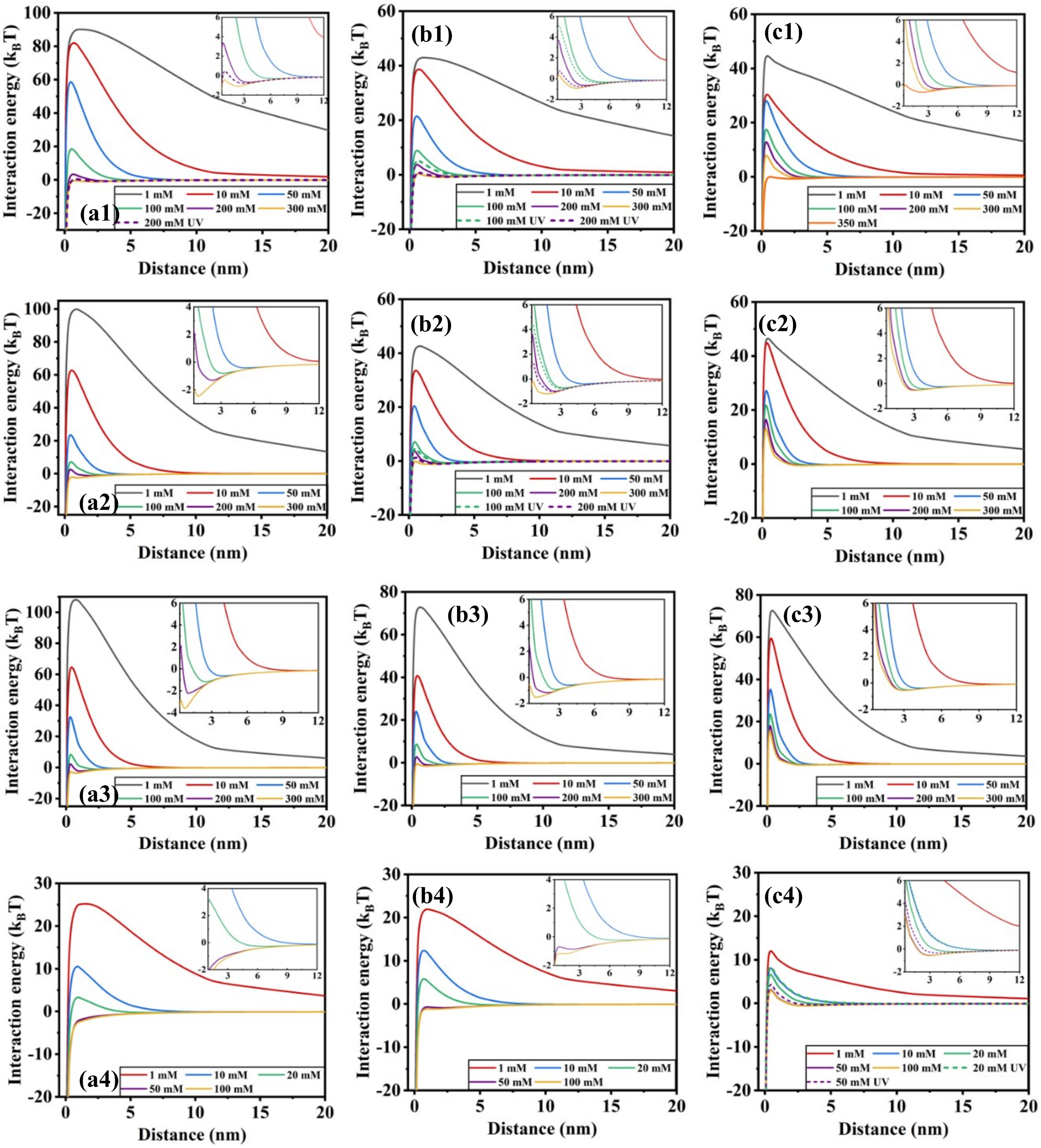

Fig. S5 Total interaction energies as a function of the separation distance between two approaching polystyrene nanoplastics (PSNPs) in different concentrations of electrolytes ("a" refers to PSNPs, "b" refers to PSNPs-NH$_2$, "c" refers to PSNPs-COOH, "1" refers to NaCl, "2" refers to Na$_2$SO$_4$, "3" refers to Na$_3$PO$_4$, and "4" refers to CaCl$_2$ solutions). The secondary minima are shown more clearly in the inset.

S6. Morphology of PSNPs-COOH in $CaCl_2$ Solution in the Dark

Twenty mL suspension of PSNPs-COOH in 20 mM $CaCl_2$ solution was sonicated in dark for 3 min and left undisturbed for 10 min. Two drops were placed onto lacey carbon support films and dried at room temperature. Then the morphology of PSNPs-COOH aggregates was observed using a Transmission electron microscopy (TEM, JEOL JSM 2100, Tokyo, Japan).

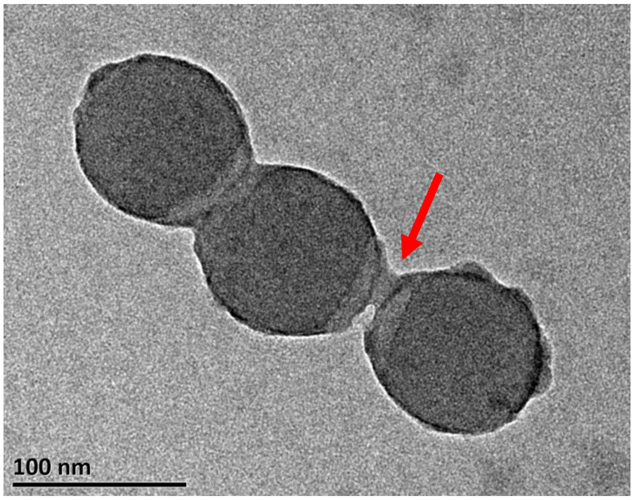

Fig. S6 TEM image of PSNPs-COOH in 20 mM $CaCl_2$ solution in the dark. Red arrow points to the bridging between carboxylate groups and calcium ion.

S7. Zeta Potentials of PSNPs before and after UV irradiation

Table S3 Zeta potentials of three PSNPs before and after 30-min UV irradiation in different electrolytes

Electrolytes		PSNPs		PSNPs-NH_2		PSNPs-COOH	
		Non-irradiated	Irradiated	Non-irradiated	Irradiated	Non-irradiated	Irradiated
NaCl	1 mM	-59.9±2.9	-57.5±4.2	-41.5±2.3	-38.6±0.5	-39.7±1.9	-40.6±4.2
	10 mM	-58.8±0.5	-54.1±3.4	-40.5±3.2	-36.7±2.4	-32.5±4.1	-33.3±1.4
	100 mM	-34.8±2.7	-31.9±2.5	-24.4±1.6	-20.3±2.1	-24.9±4.9	-26.1±1.7
	200 mM	-24.2±1.7	-19.9±2.4	-20.4±2.0	-15.6±2.1	-22.4±3.9	-25.2±3.6
Na_2SO_4	1 mM	-63.4±4.9	-61.6±2.5	-41.5±3.1	-40.9±0.2	-40.7±1.9	-42.1±2.9
	10 mM	-53.4±4.2	-55.8±1.4	-38.7±4.1	-39.8±2.6	-40.6±1.3	-42.0±1.5
	100 mM	-30.0±1.9	-29.8±1.2	-25.0±1.7	-21.9±1.7	-30.1±3.1	-30.8±2.8
	200 mM	-26.9±2.0	-23.7±3.6	-23.7±3.4	-20.1±1.2	-27.6±0.9	-28.4±1.1
Na_3PO_4	1 mM	-66.5±2.1	-65.9±0.7	-54.0±2.7	-53.8±1.4	-51.5±3.8	-52.6±1.1
	10 mM	-55.4±4.1	-54.2±1.6	-43.3±4.5	-43.2±1.0	-47.7±2.0	-48.6±1.8
	100 mM	-34.6±1.6	-33.1±1.9	-29.4±4.8	-30.8±1.7	-33.4±2.1	-35.1±3.5
	200 mM	-33.4±1.1	-32.0±4.2	-26.3±5.4	-26.1±3.6	-31.7±2.9	-32.8±2.8
$CaCl_2$	1 mM	-33.6±3.8	-34.5±3.2	-30.6±0.6	-22.4±0.5	-18.6±1.6	-19.3±1.5

	10 mM	-25.9±2.1	-25.0±0.7	-25.5±2.2	-20.2±4.1	-14.4±0.5	-15.3±2.3
	20 mM	-19.9±1.9	-19.6±2.5	-20.2±1.9	-21.2±0.5	-12.5±1.0	-14.7±1.8
	50 mM	-12.2±4.7	-12.8±2.9	-10.9±1.9	-8.73±2.47	-3.4±1.1	-7.8±1.5

S8. Effect of UV Irradiation on the Aggregation of PSNPs in Different Electrolyte Solutions

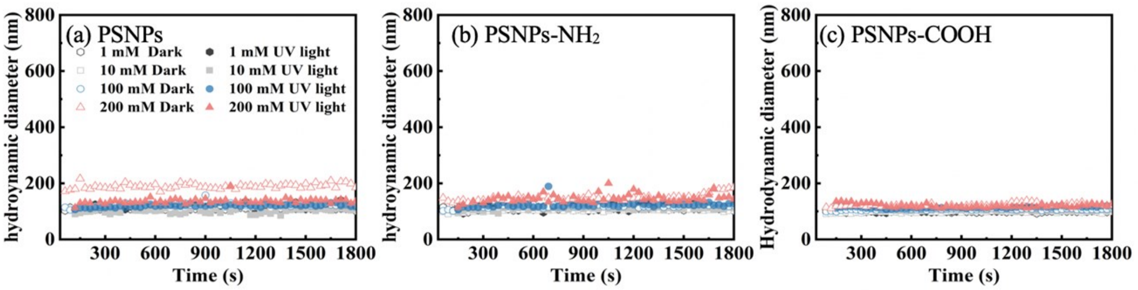

Fig. S7 Aggregation kinetics of three types of PSNPs (10 mg·L^{-1}) in different concentrations of Na_3PO_4 solutions in the dark and under UV irradiation over 30 min. The same figure legends are used for the three figures but only shown in (a).

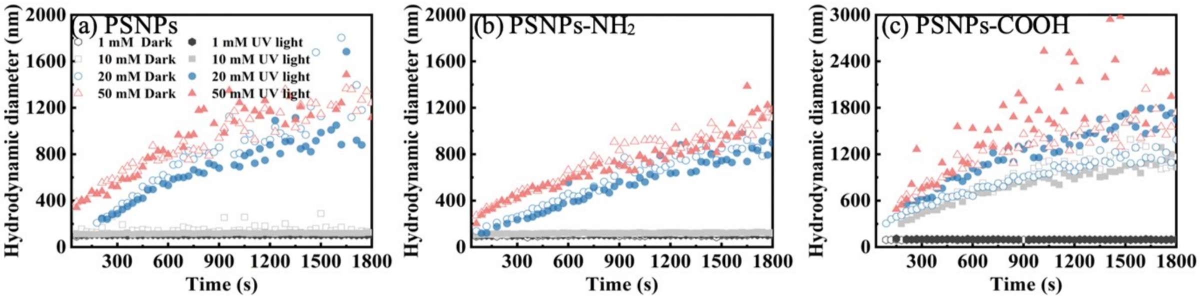

Fig. S8 Aggregation kinetics of three types of PSNPs (10 mg·L^{-1}) in different concentrations of $CaCl_2$ solutions in the dark and under UV irradiation over 30 min. The same figure legends are used for the three figures but only shown in (a).

S9. ESR Detection of $^1O_2$, •OH, and $O_2^{\bullet-}$ in DI Water under UV Irradiation

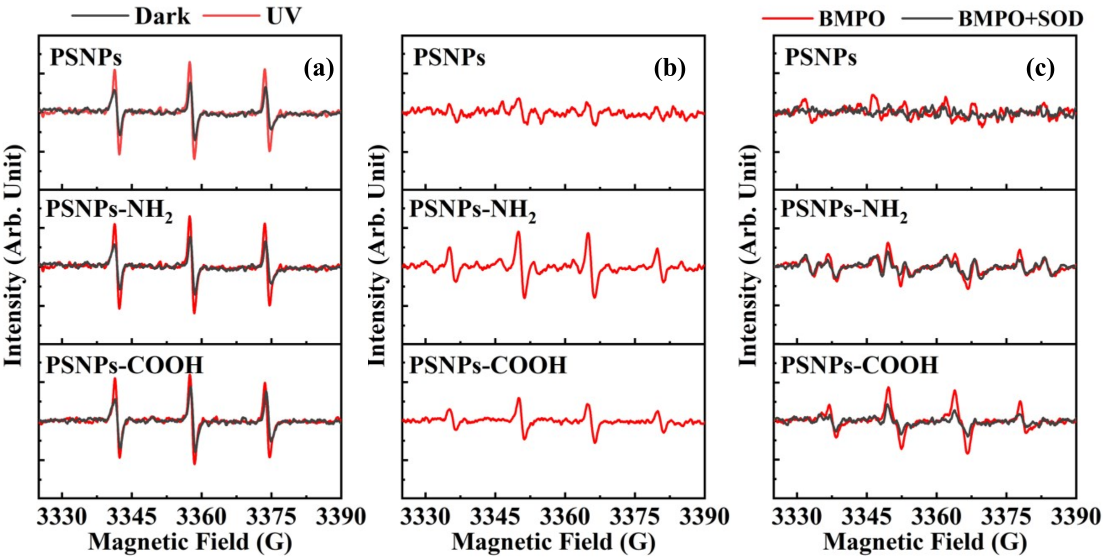

Fig. S9 ESR spectra recorded of PSNPs, PSNPs-NH_2 and PSNPs-COOH suspensions at ambient temperature for (a) TEMP adduct with $^1O_2$, (b) DMPO adduct with •OH, (c) BMPO adduct with •OH/$O_2^{\bullet-}$ before and after addition of SOD under UV irradiation.

S10. XPS of PSNPs before and after UV Irradiation

Table S4 The oxygen element contents of three PSNPs (%) before and after 30-min UV irradiation

Sample	0 h	UV irradiation	in darkness
PSNPs + 200 mM NaCl	4.62	4.07	8.06
PSNPs-NH_2 + 200 mM NaCl	7.24	7.07	8.23
PSNPs-NH_2 + 20 mM $CaCl_2$	7.24	8.24	9.61
PSNPs-COOH + 20 mM $CaCl_2$	5.19	6.38	5.95

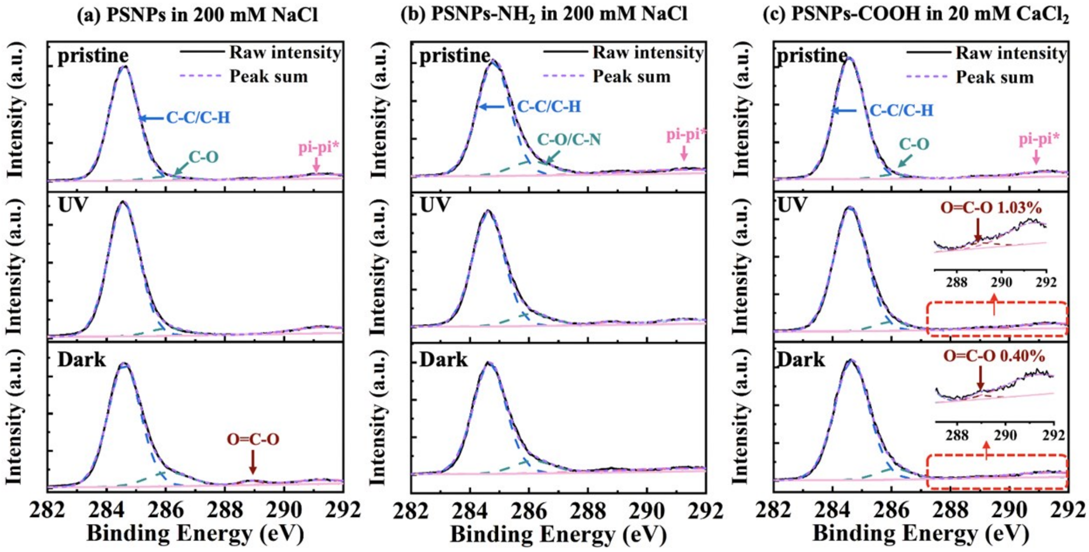

Fig. S10 The C 1s XPS spectra of (a) PSNPs in 200 mM NaCl, (b) PSNPs-NH_2 in 200 mM NaCl and (c) PSNPs-COOH in 20 mM $CaCl_2$ solution after immersion in the dark and UV exposure for 30 min.

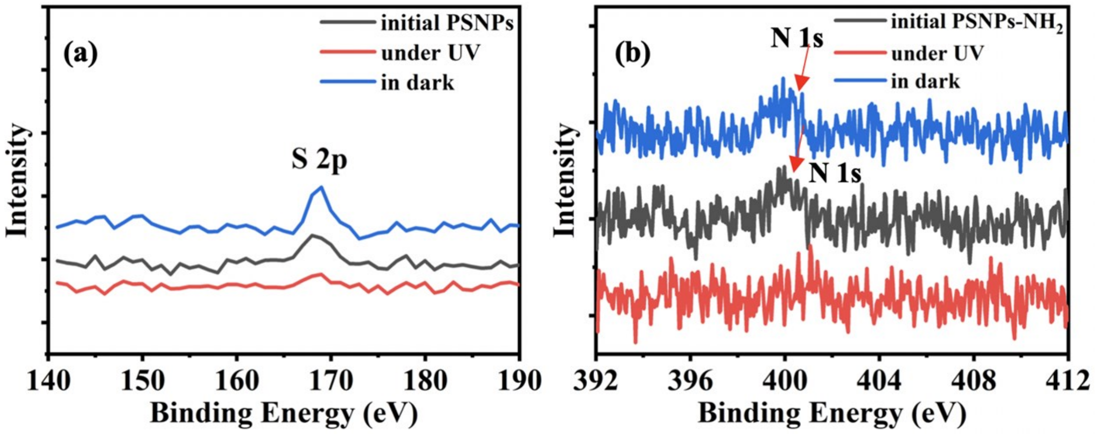

Fig. S11 (a) S 2p XPS spectra for PSNPs with or without UV irradiation in 200 mM NaCl solution. (b) N 1s XPS spectra for PSNPs-NH_2 with or without UV irradiation in 200 mM NaCl solution.

S11. UV-vis Absorbance Spectra of PSNPs in Na_3PO_4 before and after UV Irradiation

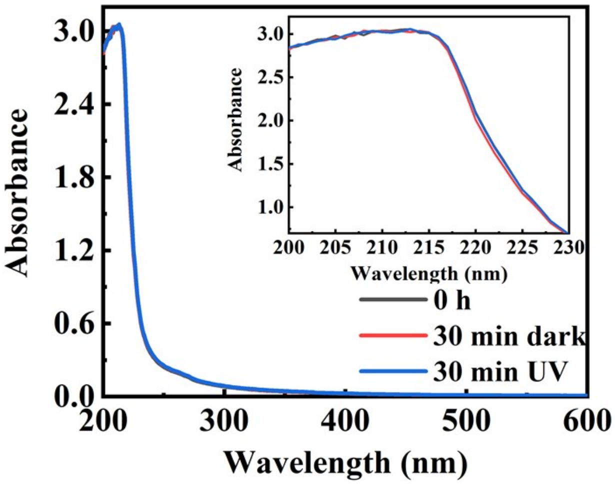

Fig. S12 UV-vis absorbance spectra of PSNPs in 200 mM Na_3PO_4. The inset shows an enlarged graph of the absorbance spectra.

S12. Hydrophilicity Transformation of PSNPs with or without UV Irradiation

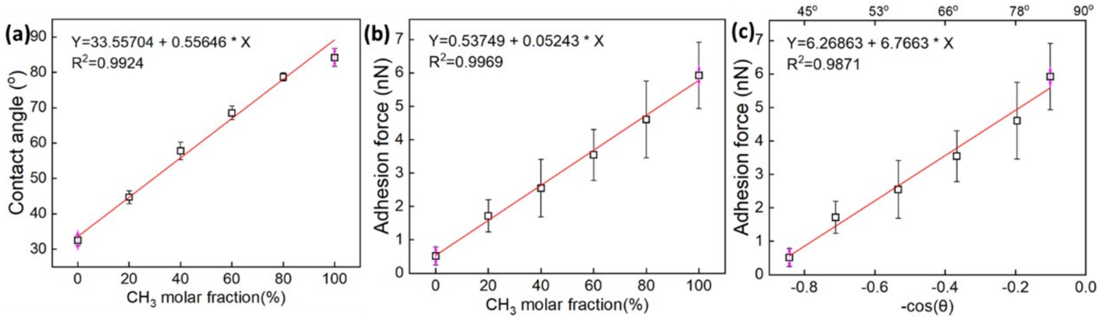

Fig. S13 (a) Water contact angle values measured for the SAM surfaces as a function of the molar fraction of CH_3; (b) Adhesion forces measured for the SAM surfaces as a function of the molar fraction of CH_3; (c) Adhesion forces versus the values of -cosθ for different SAM surfaces.

Table S5 Adhesion force measurement between CH_3-coated gold tip and PSNPs with different surface coatings in different electrolytes

Sample	Light condition	Adhesion force (nN)	Contact angle (°) calculated by mean value of adhesion force
PSNPs + 200 mM NaCl	UV light	3.59±0.40	66.7±3.7
	dark	3.45±0.42	65.4±4.0
PSNPs-NH_2 + 200 mM NaCl	UV light	1.45±0.43	44.6±5.2
	dark	1.49±0.40	45.1±4.8
PSNPs-COOH + 20 mM $CaCl_2$	UV light	1.09±0.18	40.1±2.4
	dark	1.10±0.16	40.2±2.1

Note: data of PSNPs, PSNPs-NH_2 and PSNPs-COOH in other electrolytes were not shown here, because they are similar to those in 200 mM NaCl or in 20 mM $CaCl_2$ solutions.

Reference

1. K. L. Chen and M. Elimelech, Influence of humic acid on the aggregation kinetics of fullerene (C_{60}) nanoparticles in monovalent and divalent electrolyte solutions, *J. Colloid Interf. Sci.*, 2007, **309**, 126-134.
2. C. K.L. and M. Elimelech, Aggregation and deposition kinetics of fullerene (C_{60}) nanoparticles, *Langmuir*, 2006, **22**, 10994-11001.
3. N. B. Saleh, L. D. Pfefferle and M. Elimelech, Aggregation kinetics of multiwalled carbon nanotubes in aquatic systems: Measurements and environmental implications, *Environ. Sci. Technol.*, 2008, **42**, 7963-7969.
4. J. Liu, T. Zhang, L. Tian, X. Liu, Z. Qi, Y. Ma, R. Ji and W. Chen, Aging significantly affects mobility and contaminant-mobilizing ability of nanoplastics in saturated loamy sand, *Environ. Sci. Technol.*, 2019, **53**, 5805-5815.
5. M. Giesbers, J. M. Kleijn and M. A. C. Stuart, Interactions between acid- and base-functionalized surfaces, *J. Colloid Interf. Sci.*, 2002, **252**, 138-148.
6. Y. Liu, Y. Hu, C. Yang, C. Chen, W. Huang and Z. Dang, Aggregation kinetics of UV irradiated nanoplastics in aquatic environments, *Water Res.*, 2019, **163**, 114870.
7. L. Wang, S. Xu and J. Li, Effects of phosphate on the transport of *Escherichia coli* O157:H7 in saturated quartz sand, *Environ. Sci. Technol.*, 2011, **45**, 9566-9573.
8. S. Chattopadhyay, A. Datta, A. Giglia, N. Mahne, A. Das and S. Nannarone, Intramolecular and intermolecular rearrangements in nanoconfined polystyrene, *Macromolecules*, 2007, **40**, 9190-9196.
9. D. J. Voorn, W. Ming, J. Laven, J. Meuldijk, G. de With and A. M. van Herk, Plate–sphere hybrid dispersions: Heterocoagulation kinetics and DLVO evaluation, *Colloid. Surfaces A*, 2007, **294**, 236-246.